FLAMMABILITY LIMITS OF A SOLID FUEL RAMJET COMBUSTOR

ICAS-92-7.8.2

R.F. Calzone*
Delft University of Technology
Delft, The Netherlands

Abstract

An experimental and a theoretical method to determine the flammability limits of a Solid Fuel Ramjet (SFRJ) combustor are presented in this paper. The flammability limits, obtained with the experimental method agree with the flammability limits, reported in literature. A simple numerical method, based on chemical kinetics, combustor acoustics and heat transfer by forced convection, has been developed. Calculational results show trends that are in agreement with the experimental results and the results reported in literature. Proper modelling of the heat transfer and mixing processes should prove the model's reliability in the future. From the results, it is concluded that flammability of an SFRJ combustor is primarily governed by the Damköhler first number of the gases in the recirculation zone and the amount of heat, propagated to the flow behind the recirculation zone.

I. Introduction

Solid fuel ramjets have been of interest to missile propulsion system designers for over six decennia[1,2]. Nowadays, they might also be the next generation of advanced spacecraft's propulsion systems during atmospheric flight. This is due to their large simplicity, resulting from the absence of moving parts and complex fuel supply and control systems. Furthermore, the high specific impulse (900-1000 s) results in a considerable gain in range (200-400 %) compared to a solid rocket engine of the same size and weight[1,2].

A schematic drawing of an SFRJ combustor is shown in figure 1. The solid fuel is stored in the combustion chamber and is burnt with ram air, obtained by decelerating the captured air in the inlet. In the combustor, the air mixes and reacts with the gaseous fuel. This reaction on its turn provides for the heat required to gasify the initially solid fuel. A sustained combustion process may be obtained in this way. An aft mixing chamber may be added to increase the combustion efficiency by further mixing and combustion of the unburnt gaseous fuel. Finally, the hot combustion gases are used for propulsion by accelerating them through a converging/diverging nozzle.

In general, flow rates within the combustor are high, which may cause the flame zones to be blown away. This phenomenon typically appears for all ramjets and is often referred to as blow-off or flame-out and consequently leads to mission failure. To prevent this, a device is required to stabilize a high temperature region, serving as a pilot flame.

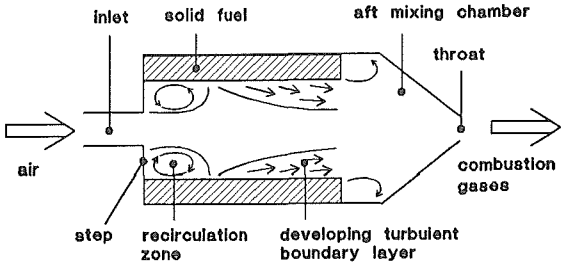

Figure 1: Typical SFRJ combustor layout.

This is accomplished by applying a sudden expansion type of combustor inlet, the step or flame holder. The highly turbulent recirculation zone created in this way, provides for a region with good mixing properties and relative low flow velocities. This results in long residence times and high gas temperatures in this region. Behind the recirculation zone, the flow reattaches and a developing turbulent pipe flow is formed.

The SFRJ combustor design is governed by opposing demands with respect to the step height. While large step heights are beneficial to flame stabilization it is desirable, from an operational point of view, to apply small step heights. For a given combustor inlet area, a maximum amount of fuel may then be stored within the combustor volume, which leads to maximum range. Another advantage of small step heights is the smaller induced pressure loss associated with the sudden expansion of the flow due to the energy associated with the induced vorticity. Finally, small step heights lead to a more uniform fuel regression, hence postponing local burn-out of the solid fuel which may lead to deteriorated performance or flame-out.

The minimum step height, required to achieve sustained combustion, has been found to primarily depend on the inlet air mass flow, the inlet temperature and the chamber pressure[3-8]. This is shown schematically in figure 2, where typical SFRJ flammability limits are shown as a function of the combustor geometry. For a specified combustor port diameter, the port over inlet area ratio A_p/A_{in} is a measure for the step height. The port over throat area ratio A_p/A_t is a measure for the mass flow over chamber pressure ratio m_{in}/p_c. The inlet conditions may vary during flight according to the operational requirements to Mach number, altitude and net thrust. This study is aimed at developing a method to determine the operational limits with respect to flame stabilization (flammability limits) of a specific SFRJ combustor.

The basics of flammability are treated in the next chapter. Then the experimental efforts to study flammability limits with the PML-TNO/FAE-DUT ramjet test facility are described. Finally, a simple model to predict the flammability limits of an SFRJ combustor is presented.

*: Student, Delft University of Technology, Faculty of Aerospace Engineering (FAE-DUT). Presently Employed by the Prins Maurits Laboratory TNO (PML-TNO)

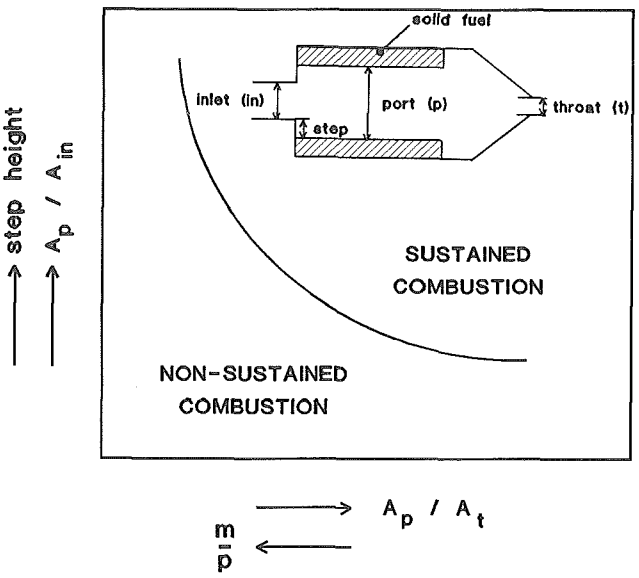

Figure 2: SFRJ combustor flammability limit.

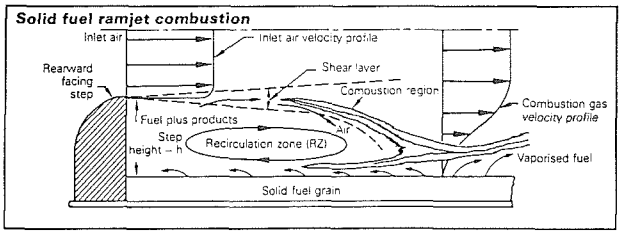

Figure 3: The SFRJ combustor recirculation zone.

II. Basics of flammability

Consider the recirculation zone, shown in figure 3. Due to the sudden expansion of the incoming air, a turbulent shear layer is formed between the main flow and the recirculation zone. The highest temperatures are found in the shear layer[9]. Part of the hot shear layer gases are captured in the recirculation zone while part of the hot combustion gases are propagated to the developing pipe flow behind the recirculation zone. In this way, the high temperature recirculation zone acts as a heat source to initialize the combustion process behind the recirculation zone. It is believed that this is the basic mechanism of flammability. For very high inlet temperatures enough heat is present in the air flow to cause self-ignition of the solid fuel and the flame holder may be omitted[3-5]. The self-ignition temperature has been found to be approximately 800 K for Polyethylene (PE) and Poly methyl methacrylate (PMMA) fuels[3-5].

According to the assumed flammability mechanism, a necessary requirement to achieve sustained combustor operation is the occurrence of combustion in the recirculation zone. In addition the temperature of the gases, propagated to the developing pipe flow, needs to be high enough ($\geq$ 800 K for PE and PMMA fuels) to sustain the combustion process behind the recirculation zone. Chemical energy is added to the recirculation zone by vaporization of solid fuel. This energy is converted from its bonded,

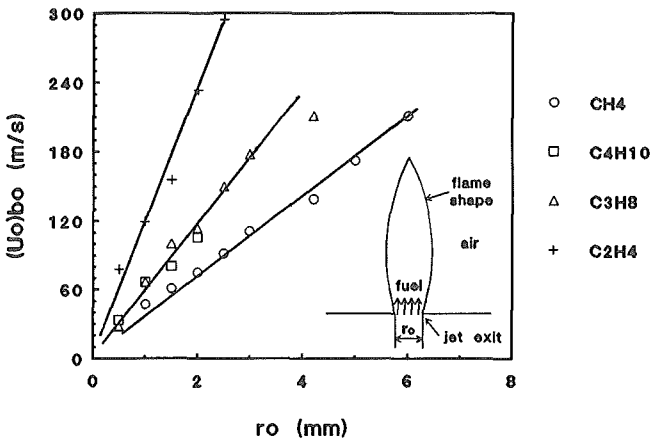

Figure 4: Blow-off velocity as a function of the flame shape parameter r_0 for several fuel types[10].

chemical, form to sensible heat by chemical reaction with the captured air. To allow for chemical reaction, the gaseous fuel is to be thoroughly mixed with the air. In addition, the reaction time needs to be smaller than the residence time of the fuel/oxidizer mixture. This is expressed by the Damköhler first number:

$$Da = \frac{mixing\ rate + reaction\ rate}{flow\ rate} \qquad (1)$$

which can also be written as:

$$Da = \frac{\tau_{res}}{\tau_{mix} + \tau_{reac}} \qquad (2)$$

where τ_{res}, τ_{mix} and τ_{reac} are the residence time, the mixing time and the time needed for reaction, respectively. The residence time is said to be long enough if Da $\geq$ 1. If Da < 1, the residence time is too short to allow for (complete) reaction.

The importance of the residence time may best be demonstrated on basis of the flame-out of a turbulent jet diffusion flame. Pitts[10] considered the flame-out mechanism for turbulent jet diffusion flames to be associated with the inability of the flame to propagate toward the jet exit. For several fuels, the blow-off velocity U_b has been found to correlate with the jet exit radius r_o. This is shown in figure 4. As the jet exit velocity is increased, the flame front is observed to be lifted off. If the jet exit velocity exceeds the blow-off velocity U_b, the flame front is blown away with the jet flow. The effect of the flame shape parameter r_o is believed to be of interest to the flammability behaviour of jet diffusion flames only and is not considered any further here. The fuel type is observed to have a prominent effect on the blow-off velocity[10], which is also reported for SFRJ combustors[3-7]. This is explained by the fact that the reaction rate is different for the several types of fuel used.

The flow within the SFRJ combustor is often treated as stationary when the interest is in the time averaged performance of the SFRJ. From experiments it is known, however, that combustion pressure and temperature histories often exhibit a rather fluctuating character. These fluctuations are accompanied by a phenomenon known as

vortex shedding, i.e. the shedding of large vortical structures from the recirculation zone. As the residence time of a hot gaseous body within the recirculation zone is determined by the frequency at which it is shed, this phenomenon is to be payed special attention to. Therefore, two models to describe the residence time are considered, including respectively the flow rate and the vortex shedding frequency.

Residence time: flow rate model

The residence time within an SFRJ combustor is determined by the time needed, for a gas particle, to travel from the combustor inlet to the combustor outlet:

$$\tau_{res} = \frac{L_c}{U_c} \tag{3}$$

where U_c is the mean gas velocity within the combustor and L_c is the combustor length. With the conservation of mass relation and the ideal gas law:

$$m = \rho\ U\ A \tag{4}$$

$$\frac{p}{\rho} = R\ T \tag{5}$$

it follows for the residence time:

$$\tau_{res} = \frac{L_c\ p_c\ A_p}{m\ R\ T_c} \tag{6}$$

where m is the mean value of the mass flow through the fuel port area A_p and p_c and T_c are the chamber pressure and the mean chamber temperature respectively. Introducing the fuel and combustion performance parameter c*:

$$c* = \frac{1}{\Gamma}\sqrt{R\ T_c} = \frac{p_c\ A_t}{m} \tag{7}$$

where Γ is the 'Vandenkerckhove' function:

$$\Gamma = \sqrt{\gamma}\ \left(\frac{2}{\gamma + 1}\right)^{\frac{\gamma+1}{2(\gamma-1)}} \tag{8}$$

and A_t is the nozzle throat area, the residence time may be written as:

$$\tau_{res} = \frac{L_c\ c*\ A_p}{R\ T_c\ A_t} = \frac{L*}{\Gamma^2\ c*} \tag{9}$$

The ratio $L^* = (L_c A_p)/A_t$ is called the characteristic length of the combustor[11]. For a given fuel, a given inlet air mass flow and disregarding large changes in the gas composition due to an altered combustor lay-out, the values of c* and Γ may be regarded as constant. The residence time is then determined by the combustor characteristic parameter L*. It is learned from equation (9) that longer residence times are achieved by increasing the combustor volume $L_c\ A_p$ or by decreasing the nozzle throat area A_t. Increasing the combustor length extends the travelling length of a gas particle at a given velocity, while increasing the port area, allows the mass to flow through it at a lower velocity. Decreasing the nozzle throat diameter, increases the chamber pressure, which enables the gas mass to pass the port area at a lower velocity. Within this view, the residence time of the gases in the recirculation zone are expected to be proportional to the recirculation zone length and inversely proportional to the mean gas flow velocity in this zone. The length of the recirculation zone has been found to be proportional to the step height h[3-5,12]. Hence, flame-out due to large flow velocities is expected for large air mass flows, low chamber pressures and small step heights. These findings are supported by results, reported in literature[3-8].

In addition, inferior flammability properties have been found for small fuel port areas[3-5]. The latter effect is explained by Zvuloni et al.[13], by the more favourable heat balance in the recirculation zone, rather than the increased residence time. For a given composition, the energy level of the reacting mixture within the recirculation zone may be expressed by the amount of heat, Q_{rz}, present in this zone:

$$Q_{rz} = c_p\ T_g\ M_g \tag{10}$$

where c_p is the heat capacity at constant pressure, and T_g is the average gas temperature. M_g is the total amount of gas mass present in the recirculation zone. For given pressure, it follows, with the ideal gas law, that the amount of heat is proportional to the recirculation zone volume. Part of this heat is required to vaporize the solid fuel, essential as a source of chemical energy. This part is equal to the heat flow from the recirculation zone to the wall. If the heat losses to the main flow and the radiative heat transfer are neglected, this heat flow is equal to the heat transfer by forced convection:

$$q_w = A_w\ h\ (T_g - T_w) \tag{11}$$

where A_w is the solid fuel wall surface, h is the heat transfer coefficient and T_g and T_w are the temperature of the hot gases and the temperature of the solid fuel wall respectively. The heat transfer by forced convection in a turbulent pipe flow is often estimated by the dimensionless correlation:

$$Nu \propto Re^n\ Pr^m \tag{12}$$

where Re, Pr and Nu are the Reynolds number, the Prandtl number and the Nusselt number of the flow, defined as:

$$Re = \frac{\rho\ U\ d_p}{\mu} = \frac{G\ d_p}{\mu} \tag{13}$$

$$Pr = \frac{c_p\ \mu}{\lambda} \tag{14}$$

$$Nu = \frac{h\ d_p}{\lambda} \tag{15}$$

In these relations, ρ, μ, λ, c_p and h represent the gas density, the dynamic viscosity, the thermal conductivity, the heat capacity at constant pressure and the heat transfer coefficient, respectively. U represents the gas flow velocity and G the mass flux through the fuel port with diameter d_p and area A_p. For fixed gas properties expressed by Pr, λ and

μ, one obtains with (12):

$$h \propto G^n d_p^{n-1} \qquad (16)$$

On comparing equally scaled combustors, i.e. with equal ratios of the port to inlet diameter d_p/d_{in}, the recirculation zone volume is proportional to d_p^3 while the wall surface is proportional to d_p^2. If, further, the combustors compared operate at the same mass flux G it follows for the ratio of the available heat and heat flow from the recirculation zone:

$$\frac{Q_{rz}}{q_w} \propto d_p^{2-n} \qquad (17)$$

Typical values for n within the range 0.6 - 0.7 were found from experimental research[3,14]. Krall and Sparrow[15] and Zemanick and Dougall[16] found n to be 2/3 for the maximum heat transfer in a separated non reacting flow. The ratio of available heat and heat flow to the wall, is larger for larger fuel port diameter. It follows that more heat is available to raise reactants to the energy level, required for reaction to occur.

Residence time: vortex shedding model

The flow within an SFRJ combustor has been found to be influenced to a considerable extent by the combustion process. Due to the coupling of the combustor acoustics to the fluid dynamics the combustor flow exhibits an oscillatory character with pressure fluctuations typically within the frequency range of 50 to 100 Hz. Van der Geld[17] investigated the oscillatory flow with combustion by studying high speed film recordings of the combustion process of a PMMA fuel. He noticed the oscillatory shedding of large-scale toroidal vortex structures in the upstream end of the fuel grain. The vortex shedding process was observed to start within the recirculation zone as shadowy spots that seemed to grow into the combustion chamber and then suddenly jump off and propagate, at a speed low compared to the main stream velocity, and diffuse in the main flow. It was found that this vortex shedding process occurs at the same frequency as the pressure and temperature oscillations and the fluctuations in light intensity. The frequencies were identified as those of the first longitudinal acoustic mode of the combustor. Other theoretical and experimental studies[18-22] reveal that the vortex shedding process is triggered by the acoustic behaviour of the combustor. The pressure oscillations associated with the vortex shedding process are driven by the combustion process. This is illustrated by Reuter et al.[22], who investigated the role of the fluid mechanics of the flame region on the driving of combustion instabilities in a ramjet engine. Measurements of the flow field behind two circular rods, serving as flame stabilizers in the premixed oxidizer/fuel flow through a 2-dimensional duct, show that the combustion process is capable of driving these pressure oscillations at the fundamental acoustic frequency of the channel. Symmetric vortex shedding occurs in the wake of the flame stabilizers. These vortices periodically distort the flame front and cause oscillatory changes in the heat release which are in phase with the pressure oscillations. In the SFRJ combustor, the oscillatory heat transfer is caused by the jump-off and diffusion within the main flow of part of the fuel rich hot gases from the recirculation zone[17].

Severe pressure fluctuations may cause damage to the structure and may increase the vehicle's drag and cause engine extinguishment due to interactions with the inlet shock system[20-21]. As will be clear from this treatment, the special problems associated with oscillatory burning may largely influence the combustor design. In this study, the interest is in the frequency, f_s, at which the vortices are shed from the recirculation zone. With the residence time being inversely proportional to the vortex shedding frequency, the Damköhler first number may also be written as:

$$Da = \frac{1/f_s}{\tau_{reac} + \tau_{mix}} \qquad (18)$$

At PML-TNO/FAE-DUT, a computer code called FRECAL has been developed to study the acoustic behaviour of a ramjet[23] and calculates the acoustic eigen frequencies of a 2-dimensional channel system, representing a ramjet layout with an injection chamber, combustor inlet, combustion chamber and aft mixing chamber. The vortex shedding frequency depends on the geometry of the channel system, and the temperatures and pressures in this system. Good agreement was found with the observations of van der Geld[17].

Reaction rate

The rates at which reactions occur have been found to be proportional to the products of the concentrations C_j, of the reacting chemical species j, each concentration being raised to a power equal to the corresponding stoichiometric coefficient, ν_j[24,25]. Thus the reaction rate is given by:

$$RR = k \prod_{j=1}^{n} (C_j)^{\nu_j} \qquad (19)$$

where k is the proportionality constant called the specific reaction rate constant and n is the total number of reacting species. For a given chemical reaction, k is independent of the concentrations C_j and depends on the temperature only. In general, k is expressed as:

$$k = A\, T^B\, e^{(-Ea/RoT)} \qquad (20)$$

This relation is called the Arrhenius law. Only those molecules which possess potential energy larger than a certain amount E_a will react and these high-energy, active, molecules lead to products[24,25]. The factor $A\,T^B$ represents the collision frequency and the exponential term is the Boltzmann factor, specifying the fraction of collisions that have an energy larger than the activation energy E_a. The values of A, B and E_a are constants for the reactions considered and are neither functions of the concentrations nor of the temperature. Due to the energy, related to the intermediate species involved, the reaction rate depends on the reaction sequence scheme considered.

The energy level of the gases in the recirculation zone, important to raise the reactants to their reactive high-energy state, is determined by the amount of heat, present in this zone. The species concentration is determined by the oxidizer/fuel mixture ratio of the reactants.

The reaction time, τ_{reac}, may be determined from calculations with the KINETICS computer code[26-29]. KINETICS calculates the temperature and composition during the combustion process of a premixed oxidizer/fuel mixture for a given mixture ratio, initial temperature and combustion pressure, based on chemical kinetics. KINETICS uses a chemical kinetic database in which the Arrhenius coefficients are stored.

Mixing

In a turbulent flow, the mass exchange across a stream line is governed by the turbulence level of the flow. Mixing may be improved by increasing the turbulence level of the incoming flow[30]. Jones[31] and Boaz[32] report that the turbulence level of the incoming sudden expansion flow, expressed by the turbulent kinetic energy, is a function of the Reynolds number, based on the step height h:

$$(\frac{v'}{U})^2 = f(Re)_h \qquad (21)$$

where:

$$(Re)_h = \frac{U_{in}\ \rho\ h}{\mu} \qquad (22)$$

With the conservation of mass law it follows:

$$(Re)_h = \frac{m_{in}\ h}{A_{in}\ \mu} \qquad (23)$$

Thus, good mixing is achieved by increasing the step height and increasing the inlet air mass flow.

III Experimental investigation

In this chapter, the flammability limits of an SFRJ combustor are investigated experimentally with the PML-TNO/FAE-DUT ramjet test facility. It is aimed to develop a procedure to determine the flammability limits, thus extending the available experimental data on flammability.

Test facility

At PML-TNO/FAE-DUT the internal ballistics of an SFRJ combustor have been investigated thoroughly[33,12,14,17], using the connected pipe type of ramjet test facility, shown schematically in figure 5.

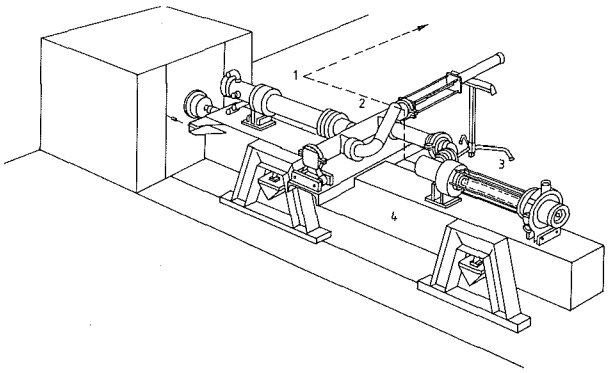

Figure 5: PML-TNO/FAE-DUT ramjet test facility.
1. Vitiator.
2. Three way valve.
3. SFRJ combustor.
4. Thrust bench.

Air may be supplied up to a maximum mass flow of 5 kg/s from a pressurized storage vessel. The air may be heated in a vitiator by combustion of methane with this (oxygen enriched) air, up to a maximum temperature of 1000 K[34]. In the injection chamber, hydrogen and oxygen are mixed with the (hot) air flow and ignited by a spark plug. The hot flame, obtained in this manner, serves as an ignition torch when the shuttle valve is opened towards the combustion chamber and is taken along with the air flow. The combustion chamber consists of a cylindrical fuel grain. The inlet is formed by a diaphragm. An aft mixing chamber is added to increase the residence time and hence combustion efficiency. Several diaphragm and nozzle inserts are available. This allows for performing 'go/no-go' type of tests for a wide range of values of A_p/A_{in} and A_p/A_t. The air mass flow is controlled by a Sonic Control and Measuring Choke (SCMC), being an especially developed computer controlled flow meter which guarantees a constant mass flow rate[35]. At several spots, the temperature and pressure are measured, using thermocouples and piezo electric pressure transducers, respectively.

A computer programme, especially developed at PML-TNO, accounts for data acquisition, processing and representing data. The tests may be recorded with a video recorder to enable repeated observation and comparison of the several tests.

Criteria for sustained combustion

To determine whether or not sustained combustion takes place after ignition, it is necessary to define combustion criteria. A measurable criterion for sustained combustion is derived using the characteristic velocity with its limit value for sustained combustion based on the self ignition temperature of 800 K observed for PE and PMMA (see chapter II). From calculations with the NASA SP-273 computer code[36], a value of c* = 720 m/s at an adiabatic flame temperature of 800 K was found for the combustion of PE with air. For a non-sustained combustion process, a value of c* = 420 m/s follows from relation (7), taking T_c = 290 K and γ = 1.4. The corresponding chamber pressure, p_{air}, may be used as a quick check upon an assumed non-sustained combustion process, during testing. In addition, the emission of light is considered as a criterion for sustained combustion. If no light is emitted at the end of the self-sustained phase, the combustor is believed to exhibit flame-out.

The combustion process may additionally be characterized by a combustion quality factor defined as:

$$\xi = \frac{(c*)_{exp}}{(c*)_{th}} \qquad (24)$$

where $(c^*)_{exp}$ is the experimentally determined value of c*, which will be treated later, and $(c^*)_{th}$ the theoretically predicted value of c*. The value of $(c^*)_{th}$ is determined as a function of the mixture ratio with the NASA SP-273 computer code[36]. Since the effect of the ignition process on the fuel mass reduction is not known, the mixture ratio cannot be determined from the experiments. Instead, an empirical relation, for the average regression rate dependence on the mass flow is used to estimate the fuel regression rate r[14]. The fuel mass flow then follows from:

$$m_f = r\,\rho\,A_w \qquad (25)$$

where ρ is the fuel density and A_w is the wall area. The mixture ratio Φ then easily follows from:

$$\Phi = \frac{m_{in}}{m_f} \qquad (26)$$

where m_{in} is the inlet air mass flow.

Ignitability

Special limits are formed by the inability of the igniter to start the combustion process. These limits are referred to as the ignition limits of the igniter/combustor combination. From the self-ignition temperature, T_{si} = 800 K, it is expected that no ignition will be achieved below an ignition gas temperature of 800 K.

To calculate the ignition gas temperature, the theoretical adiabatic flame temperature of the H_2/O_2/Air mixture, serving as an ignition torch, has been calculated with the NASA SP-273 computer code[36] as a function of the total mixture ratio. This mixture ratio is calculated from:

$$\Phi_{ign} = \frac{m_{air} + m_{O_2}}{m_{H_2}} \qquad (27)$$

The H_2 and O_2 mass flows were set respectively to 3 g/s and 31 g/s for all tests.

Test parameters and test conditions

It is not aimed to investigate the effects of all parameters on flammability. Instead, it was decided to perform burning tests for one fuel type, one nominal combustor port diameter and one value of the inlet air temperature. Thus, only one line in the A_p/A_{in} vs. A_p/A_t graph is determined (see chapter I). The test conditions are shown below:

Fuel	= Polyethylene
p_c	= 0.5 MPa
$(T_t)_{in}$	= 290 K
d_p	= 45 mm
L_{grain}	= 300 mm

The grain length is mentioned because of its appearance in later calculations only, while its effect on flammability will not be investigated.

As the value of A_p/A_t is a measure for the chamber pressure to mass flow ratio p_c/m, the value of the chamber pressure still is a function of the mass flow at each point in the A_p/A_{in} vs. A_p/A_t graph. The pressure effect on flammability was excluded, initially, by performing the tests at approximately one pressure level. Three tests were repeated with a higher inlet air mass flow, to examine the effect of a larger chamber pressure for the same geometric conditions and the same chamber flow velocity, i.e. the same ratio p_c/m_{in}.

To examine the effect of the flow velocity on flammability, the air flow velocity at the combustor inlet, U_{in}, is calculated. Similar to the results, obtained by Pitts[10], for the blow-off velocity of the turbulent jet diffusion flame, the residence time in the recirculation zone is assumed to be inversely proportional to the inlet flow velocity, which is easily determined from the injection chamber pressure and temperature, the inlet air mass flow and the inlet diameter. The residence time is also assumed to be proportional to the step height (see chapter II). It follows, that the non-sustained combustion experiments are expected for large values of the ration U_{in}/h.

Testing procedure

The tests performed are of the 'go/no-go' type. After ignition, the combustion process is left to itself. The following procedure has been used:

t = 0 s :	Start of air, and H_2/O_2 igniter flows. Ignition of this mixture with a spark plug.
t = 4 s :	End of ignition, H_2 and O_2 flows are terminated.
t = 8 s :	End of experiment, air flow is terminated.

After each test, it was determined whether sustained combustion was obtained (between t = 4 s and t = 8 s) or not, based on the criteria introduced before. Then new test conditions were defined, depending on the location of the flammability limit, determined by the current experiments and the flammability limit expected from literature. For a chosen value of A_p/A_t, the desired chamber pressure is obtained by setting the inlet air mass flow according to the following relation:

$$m_{in} = f_1 \frac{p_c A_t}{c^*} \qquad (28)$$

The factor f_1 is an empirical correction factor, to account for the fuel mass flow. The fuel mass flow has been found to be approximately 5 % of the total mass flow, for a wide range of mass flows[14]. Therefore, a value f_1 = 0.95 has been taken for all experiments. The value of c* in relation (28) is obtained from the predicted value of the oxidizer/fuel mixture ratio, using the NASA SP-273 computer code[36]. The mixture ratio is approximated with:

$$\Phi = \frac{m_{in}}{\bar{r}\,\pi\,d_p\,L\,\rho} \qquad (29)$$

where $\bar{r}$ is the mean regression rate, d_p is the fuel port diameter, L is the fuel grain length and ρ = 940 kg/m^3 is the fuel density. The mean regression rate may be calculated from the following empirical relation, neglecting the effect of step height variation on the regression rate[14]:

$$\bar{r} = 6.09.10^{-6}\,\bar{G}^{0.6938} \qquad (30)$$
$$(0.4\ MPa < p_c < 0.5\ MPa)$$

where $\bar{G}$ is the mean total mass flux in kg/m^2-s and $\bar{r}$ is in m/s.

After each test, the value of c* is calculated from:

$$c^* = \frac{p_c A_t}{f_2 \frac{\Delta M}{t_b} + m_{in}} \quad (31)$$

where p_c is the average chamber pressure measured during the self-sustained phase. The first denominator term accounts for the fuel mass flow during the self-sustained phase. ΔM is the fuel mass reduction during the burning time t_b, determined after each test by weighing the fuel grain. The factor f_2 corrects for the fuel mass flow during ignition. Values for f_2 within the range 0.67 - 0.80 are found from regression rate measurements. A value of f_2 = 0.70 has been taken for all tests.

Data reduction

Due to the combustion process, the pressure level is raised above the value of p_{air}. The burning time is defined as the time interval during which the chamber pressure p_c is higher than the value of p_{air}. The self-sustained chamber pressure was defined as the chamber pressure at the end of the self-sustained phase. The injection chamber flow properties were determined in a similar way. If the injection chamber flow velocity is neglected, the inlet flow velocity and Mach number follow from these total inlet conditions from the conservation of mass law, the Poisson relations and the ideal gas law, taking γ = 1.4 and R = 290 J/kg-K.

The length of the recirculation zone L_{rz} is determined by the point of maximum diameter, $(d_p)_{max}$. This point is determined from grain profile measurements.

Results and discussion

The theoretical values of T_{ign} are shown for each test in figure 6. For test number 22, no ignition was achieved, which is explained by the low ignition gas temperature T_{ign} = 600 K. For test number 11 and 23, adiabatic flame temperatures of 815 K, slightly higher than the self-ignition temperature, were calculated. Immediate flame-out after ignition has been observed for these experiments, which might be explained from a shortage of ignition power.

Figure 7 shows the value of c* for each test. The presumed sustained combustion limit c* = 720 m/s and the theoretical value for cold air c* = 420 m/s are indicated in the figure. It is noted, that the value of c* may become lower than the predicted theoretical value of c* = 420 m/s. This is explained by the fact that the flow velocity is neglected and by the error in the determination of c*. It is learned that the value of c* varies between 400 m/s and 1000 m/s. It follows that the sustained combustion region is not determined by a steep drop of c*. Instead, the gradual decrease of c* indicates a gradual transition from sustained combustion to non-sustained combustion. The intermediate region will be indicated as partially sustained. From visual observations, it was learned that the experiments designated as partially sustained exhibit light emission in an upstream part of the fuel grain only, with a minimum equal to the length of the recirculation zone. The latter is shown as a function of the step height in figure 8. The following linear best-fit relation between the length of the recirculation zone is found:

$$L_{rz} = -11.5 + 9.7\,h \quad (32)$$

All data lie between L_{rz}/h = 8 and L_{rz}/h = 10, which is in agreement with the results obtained by other investigators[3-5,12]. The findings that combustion behind the recirculation zone takes place for all experiments, exhibiting combustion in the recirculation zone, is in agreement with the adopted flammability mechanism, stating that the recirculation zone serves as a pilot flame for the flow behind the recirculation zone. On combining the combustion criteria, a critical value of c* = 770 m/s for sustained combustion is found.

Two types of combustion are illustrated on basis of the photographs shown in figure 9. In figure 9.a, a sustained combustion process with light emission along the full length of the fuel grain is shown. Figure 9.b shows a combustion process with light emission in an upstream part of the fuel grain only, the partially sustained combustion process. Flame-out was observed to take place as a quick draw-back of the combustion zone towards the step. Some of the experiments exhibited a rather fluctuating combustion process, characterized by the occurrence of alternating dark and bright zones, which were observed to travel downstream.

The resulting flammability limits are shown in figure 10 and compared with the results from literature[3-5], obtained by interpolation, in figure 11. The limit between the sustained and partially sustained region is indicated as the sustained flammability limit. The limit between the non-sustained and the partially sustained region is indicated as the non-sustained flammability limit. Agreement with the expected results from literature is found.

In figure 12, lines of constant value of the combustion quality factor ξ are shown in the A_p/A_{in} vs A_p/A_t graph. It is learned that the value of ξ gradually increases towards the region of sustained combustion, indicating the gradually improving combustion process.

The pressure and air mass flow regimes are shown in figure 13. For fixed value of A_p/A_{in}, the chamber pressure is observed to decrease with increasing inlet air mass flow, due to the deteriorating combustion process.

To examine the effect of a larger chamber pressure for the same geometric conditions and the same flow velocity, i.e. the same ratio p_c/m_{in}, 3 tests were repeated with a higher inlet air mass flow. For the respective experiments, no effect on flammability was noticed. Apparently, increasing the chamber pressure by increasing the inlet air mass flow, has no effect on the combustor flammability limits. This may be explained by the effect of mass flow and chamber pressure on flammability being basically the same through their opposite effect on the residence time (eq. 6). It results that the flow velocity remains approximately constant for increased inlet air mass flow. The calculated value of the inlet flow velocity is shown as a function of the initial step height in figure 14. For step heights larger than 13 mm, the inlet is choked and the inlet flow velocity is not further increased by the increased inlet air mass flow. At each step height, the combustion process is observed to deteriorate with increasing inlet flow velocity. Very similar to the

results, obtained by Pitts[10] for the blow-off velocity of a turbulent jet diffusion flame, the non-sustained limit is formed by a line with constant step height over inlet flow velocity ratio. These results do support the adopted flammability mechanism, stating that flame-out occurs due to a shortage of residence time. If this flammability mechanism is correct, flame-out at low values of A_p/A_{in} is explained by a shortage of residence time due to the small step height. Flame-out at low values of A_p/A_t may then be explained by the increased flow velocity resulting from the increased mass flow at constant chamber pressure. As only few non-sustained tests are performed, further investigation of the combustion process on the flow rate is recommended.

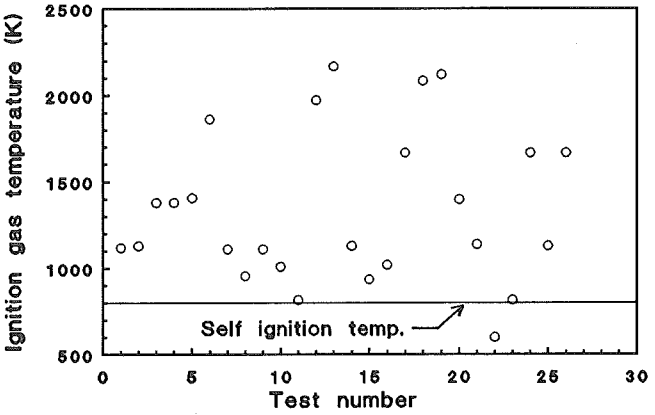

Figure 6: Ignition temperature for each test.

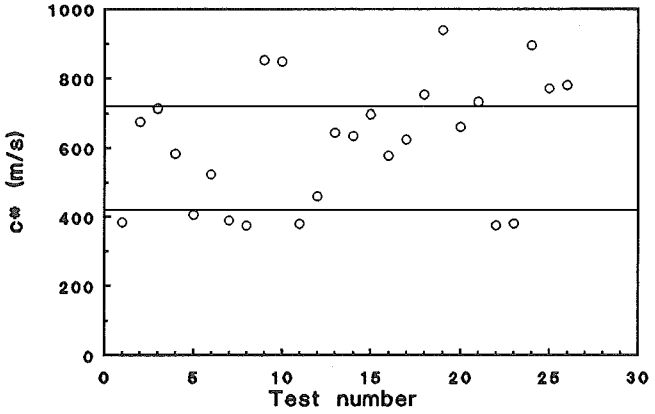

Figure 7: Characteristic velocity for each test.

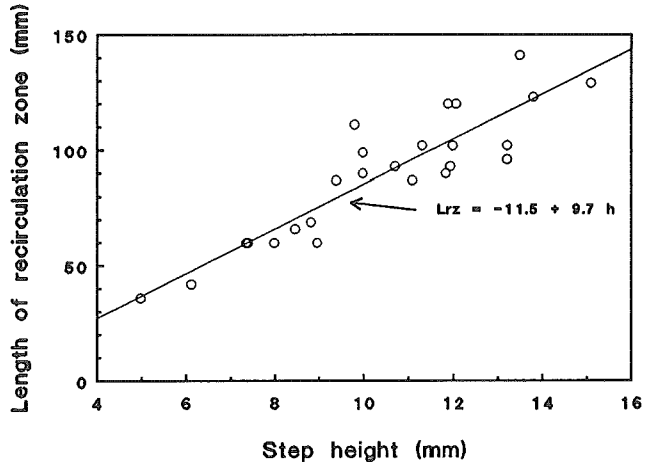

Figure 8: Reattachment length as a function of the step height.

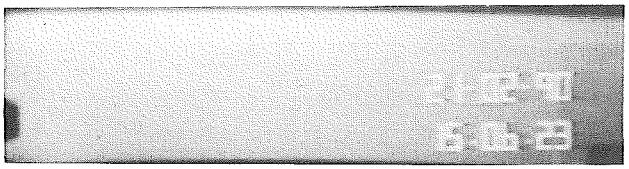

a: Sustained combustion.

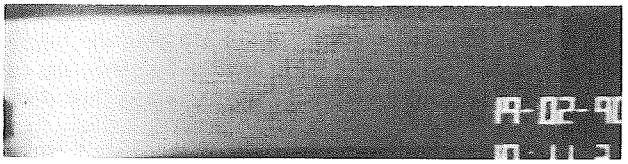

b: Partially sustained combustion.

Figure 9: Types of combustion, light emission results.

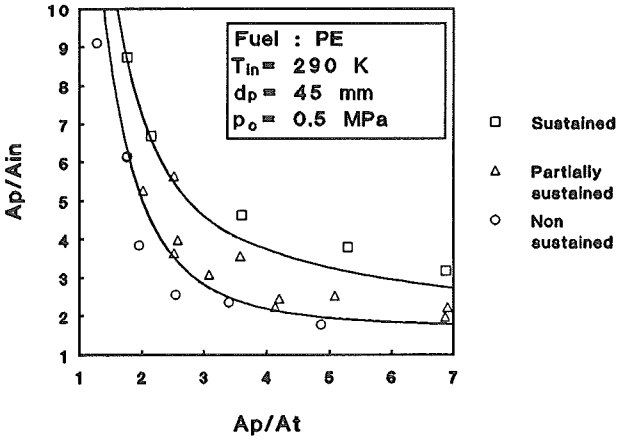

Figure 10: Resulting flammability limits.

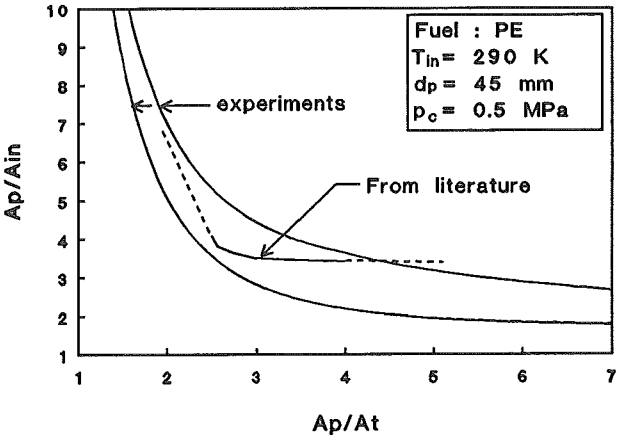

Figure 11: Comparison of experimental results with results expected from literature.[3-5]

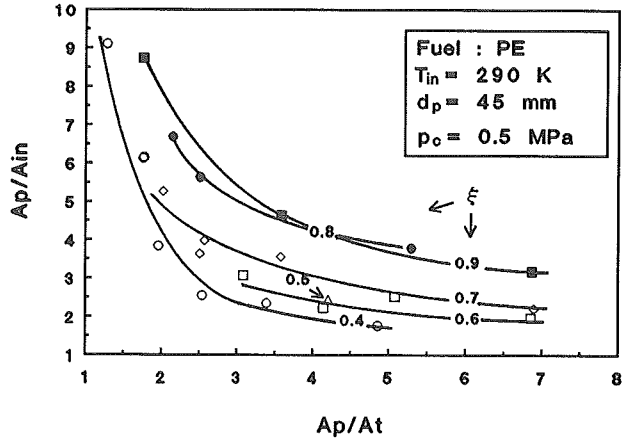

Figure 12: Lines with constant values of the combustion quality parameter ξ.

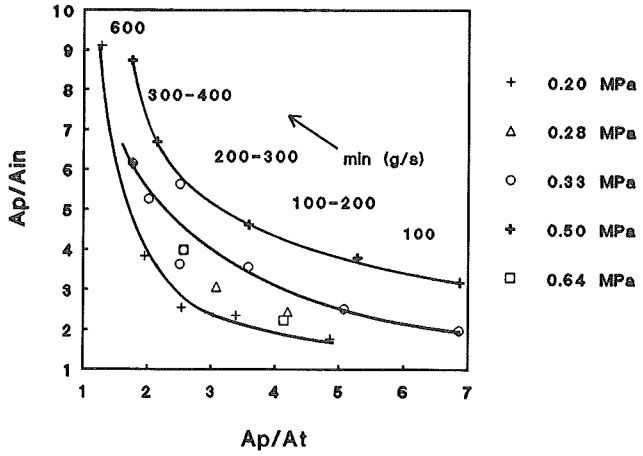

Figure 13: Constant pressure lines for different air mass flow regimes.

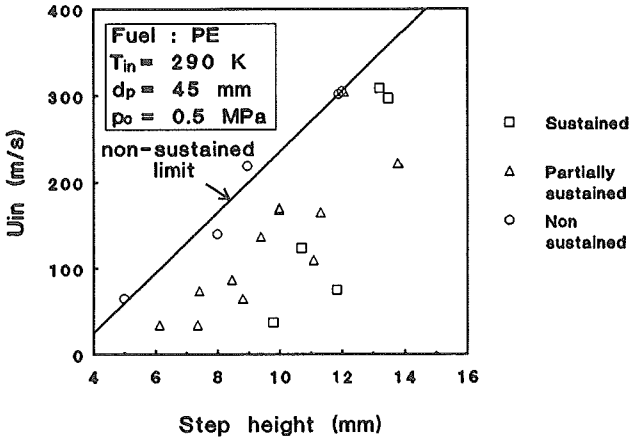

Figure 14: Inlet flow velocity as a function of the step height.

IV Modelling flammability

In this chapter, a simple flammability model is presented. The purpose is to investigate the feasibility of this model to predict the flammability limits of an SFRJ combustor in order to reduce the number of (expensive) tests.

Assumptions

To ease the modelling of flammability, some assumptions are made. First, the gases are treated as ideal and hence are assumed to obey the ideal gas law. The thermodynamic and transport properties of an ideal gas may be subdivided in frozen gas properties and equilibrium gas properties. In the case of frozen gas properties, the chemical reactions are assumed to be infinitely slow; the gas composition does not change due to a change in gas temperature and pressure. In the case of equilibrium gas properties, the chemical reactions are assumed to be infinitely fast and the gas composition changes instantaneously with changes in temperature and pressure. In the latter case, the thermodynamic and transport properties have to be corrected for the energy associated with a change in the state of equilibrium[37]. Only equilibrium properties are considered in the present modelling. Finally, mixing is neglected which means that the recirculation zone is treated as a well-stirred reactor.

The flammability model proposed here is based on the assumed mechanism of flammability, discussed in chapter II. Regarding the experimental results, two flammability limits may be distinguished, the lower or non-sustained limit, associated with flame-out of the recirculation zone, and the upper or sustained limit, associated with flame-out of the combustor. Both are considered below.

Flammability of the recirculation zone

With the assumption that the recirculation zone acts as a well-stirred reactor, the criterion for sustained combustion in the recirculation zone is formulated as:

$$Da_{rz} = \frac{\tau_{res}}{\tau_{reac}} > 1 \qquad (33)$$

The residence time may be written as the reciprocal of the vortex shedding frequency f_s:

$$\tau_{res} = \frac{1}{f_s} \qquad (34)$$

The oscillatory shedding and refilling of part of the recirculation zone is translated into a dual time-step model, explained on basis of figure 15. Assume a gaseous recirculation zone with mixture ratio Φ_1 and temperature T_1. At the beginning of the first time step, at t = 0, a fraction k is shed from the volume of the recirculation zone and re-filled with cold air. At the beginning of the second time step, at $t = 1/2f_s$, the cold air mixes with the remainder of the hot gas to form a homogeneous gaseous body with mixture ratio Φ_2 and initial temperature T_{2i}. At $t = 1/f_s$, again a fraction k of the recirculation zone volume is shed and mixing with cold air takes place at $t = 3/2f_s$. The mixture may or may not ignite and fully react during the time interval confined by $t = 1/2f_s$ and $t = 3/2f_s$, depending on the initial temperature T_{2i} and the mixture ratio Φ_2. If, at the assigned chamber pressure p_c the initial temperature is too low for reaction to occur within the residence time, $1/f_s$, or: $(\tau_{reac})_{pc,Ti} > 1/f_s$, the recirculation zone exhibits flame-out.

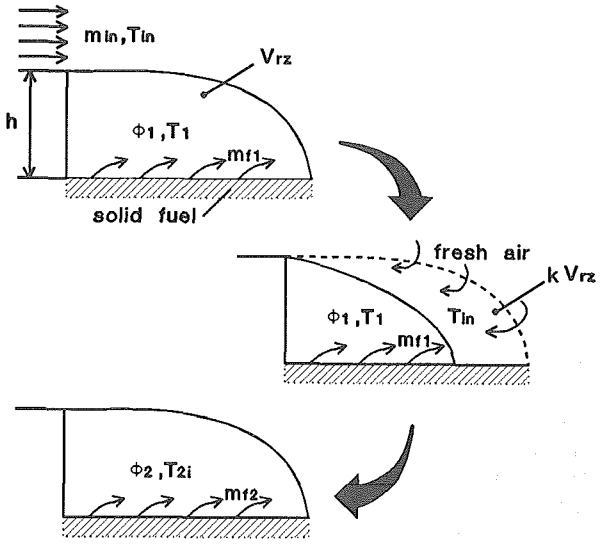

Figure 15: Dual time-step model.

It should be noted that in the preceding, the following assumptions are made. First, the two time steps are assumed to be of equal duration, i.e. $1/2f_s$ sec. Secondly, the mixing is assumed to take place in an infinitely short time interval at $t = 1/2f_s$ sec. This assumption results from the recirculation zone being treated as a well stirred reactor. Finally, each cycle, a fixed fraction k of the recirculation zone is shed. This fraction probably depends on the acoustics and the combustion process itself, due to the induced variation of the density caused by the variations in heat release. It is clear that, within this model philosophy, the combustion ceases if $k = 1$, since all the hot gases are shed and refreshed with cold air in this case. The sensibility of the model results with respect to this factor will be discussed later. Corrections for these assumptions can be made only if the mixing and vortex shedding process can be properly modeled. This, however, leads beyond the intentions of the model presented in this work.

The vortex shedding frequency was determined as a function of the mean chamber and inlet temperatures and pressures, and the combustor geometry, expressed by the ratio A_p/A_{in} and the port diameter d_p, using the FRECAL computer code[23]. The value of τ_{reac} was calculated as a function of the initial temperature T_i and the chamber pressure p_c, using the KINETICS computer code[27]. The initial temperature is calculated with relation (35). The chamber pressure is to be specified in the current model. For reasons of simplicity, the available calculations at an equivalence ratio $\phi = 1$ were used in the present modelling. For values of ϕ above 10 or below 0.1, corresponding to values of Φ above 140 and below 1.4 for a ethylene/air mixture, the reaction time may quickly increase. These extreme values of the mixture ratio are not expected, however. The value of T_i, resulting from mixing of the captured air with temperature T_{in} and the hot gases in the recirculation zone with temperature T_{rz}, follows from the conservation of energy:

$$-\int_{Trz}^{Ti} [\sum_{j=1}^{n} m_j (c_p)_j]_g \, dT = \int_{Tin}^{Ti} m_{air} (c_p)_{air} \, dT \qquad (35)$$

If it is assumed that the composition of the mixture remains constant (frozen composition), relation (35) can be solved iteratively for T_i, if the relations between the specific heats and the gas temperature are known for each species. If equilibrium composition is assumed, the energy associated with the changed composition and the heats of formation and reaction are to be taken into account and solving of (35) for T_i will be more difficult and requires the calculation of the gas properties during the mixing process. Both methods of determining T_i are beyond the intention of this research. If it is assumed that the value of c_p is constant, and independent of the temperature, the initial temperature is simply determined by weighing the inlet air temperature, T_{in}, and the recirculation zone gas temperature, T_{rz}, with the factor k:

$$T_i = (1-k)\, T_{rz} + k\, T_{in} \qquad (36)$$

In the current model, the inlet air temperature is to be assigned, while the recirculation zone gas temperature is calculated as a function of the recirculation zone mixture ratio Φ_{rz} and the inlet air temperature T_{in}, using the NASA SP-273 programme[36]. The recirculation zone mixture ratio follows from the air mass flow captured in the recirculation zone, $(m_{in})_{rz}$, and the fuel mass flow from the solid fuel wall in the recirculation zone, m_f:

$$\Phi_{rz} = (\frac{m_{in}}{m_f})_{rz} \qquad (37)$$

Flammability of the whole combustor

The criterion for sustained combustion of the whole combustion chamber follows from the self-ignition temperature T_{si} of the fuel:

$$T_c > T_{si} \qquad (38)$$

where T_c is the chamber gas temperature. The chamber gas temperature is determined as a function of the mean chamber mixture ratio, Φ_c and the inlet air temperature T_{in}, using the NASA SP-273 computer code[36]. The mean chamber mixture ratio is determined from the inlet air mass flow and the fuel vaporization in the recirculation zone:

$$\Phi_c = \frac{m_{in}}{m_f} \qquad (39)$$

In addition, complete mixing of these reactants is assumed.

Model parameters

From the preceding, it is clear that the effort of the current modelling is to determine the mixture ratio in the recirculation zone and the mean chamber mixture ratio. This is shown schematically in figure 16. The fuel mass flow follows from the heat flow q_w through wall area A_w and the heat of gasification h_v:

$$m_f = \frac{q_w A_w}{h_v} \qquad (40)$$

The wall area can be calculated if the length of the recirculation zone L_{rz} is known, from:

$$A_w = \pi\, d_p\, L_{rz} [\frac{1}{2}(1 - k) + \frac{1}{2}] \qquad (41)$$

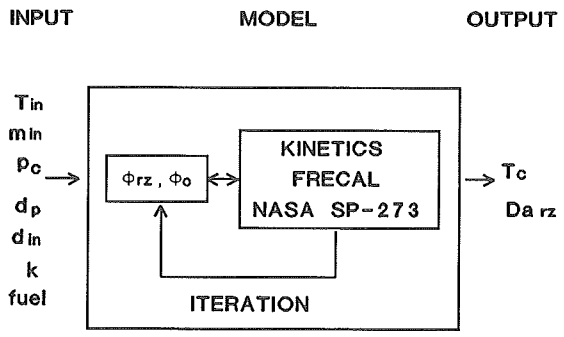

Figure 16: Schematical model.

where the term between brackets accounts for the length of the recirculation zone, being shortened to (1-k) times its length during half a vortex shedding cycle and being stretched again to its full size during the other half of the vortex shedding cycle. The length of the recirculation zone is determined from the experimentally obtained relation (32). The heat of gasification has been investigated by de Wilde[38] and is shown in table 1 for polyethylene as a function of the wall temperature. The values in this table follow from pyrolysis models and may not be regarded as absolute values. The mean of the linear and branched values shown, are used in the current model.

Table 1: Heat of gasification according to de Wilde[38]

	h_v [kJ/kg]	
T_w [K]	Linear PE	Branched PE
700	5165	5315
750	5320	5535
800	5475	5775
850	5635	6045

The heat flow per unit area q_w follows from relation (11). The wall temperature lies within the range of 600 - 800 K[38]. To determine the heat transfer coefficient h, the dimensionless Nusselt number is used (eq 15). The Nusselt number of a fluid in a channel with a sudden expansion has been determined by Krall and Sparrow[15] and Zemanick and Dougall[16]. They found that the Nusselt number is a function of the Reynolds number of the fluid based on the inlet diameter. For the peak Nusselt number, occurring at the point of reattachment, the following relation holds:

$$Nu_{max} = 0.2\ (Re_{in})^{0.66} \qquad (42)$$

The mean nusselt number, $\bar{Nu}$, in the separated region between combustor inlet and reattachment point is about 5/6 Nu_{max}, with which the heat transfer coefficient can be written as:

$$h = \frac{\bar{Nu}\ \lambda}{d_p} = \frac{(Re_{in})^{0.66}\ \lambda}{6\ d_p} \qquad (43)$$

The only unknown parameter is the thermal conductivity λ which is determined as a function of the recirculation zone mixture ratio, using the NASA SP-273 computer code[36].

The air mass, captured in the recirculation zone, is determined from the fraction k that is shed f_s times each second from the recirculation zone volume V_{rz}. If this fraction is assumed to be refilled with fresh air, the air mass flow to the recirculation zone can be written as:

$$(m_{in})_{rz} = k\ V_{rz}\ \rho_{air}\ f_s \qquad (44)$$

The volume of the recirculation zone follows from observations that the recirculation zone forms a quarter of an ellipse with the length of the recirculation zone and the step height as its sides[17]. Thus, the volume of the recirculation zone is formed by the volume inclosed by rotation of the quart elliptical contour around the central axis of the combustor:

$$V_{rz} = \frac{1}{4}\ \pi^2 d_p\ h\ L_{rz} - \frac{2}{3}\ \pi\ h^2\ L_{rz} \qquad (45)$$

The density of the cold air follows from the combustor inlet temperature and the chamber pressure, according to the ideal gas law.

Finally, the value of the characteristic velocity is calculated from the mean chamber mixture ratio, using the NASA SP-273 computer code[36]. This allows for calculation of the throat area, using relation (7). The regression rate is calculated from:

$$r = \frac{m_f}{\pi\ d_p\ L_{rz}} \qquad (46)$$

Results and discussion

In figure 17, the flammability limits for d_p = 45 mm and k = 0.5 are compared with the experimentally found flammability limits and results obtained with the COPPEF code[39], developed at PML-TNO/FAE-DUT to study turbulent reacting flows on basis of chemical kinetics. It is learned from this figure that, in contradiction to the experimental results, a minimum value of A_p/A_t occurs for the non-sustained limit. For values of A_p/A_{in} higher than 5, larger values of A_p/A_t are needed to prevent flame-out of the recirculation zone. Probably this is a result of the heat transfer being overpredicted at large values of A_p/A_{in} which leads to an overprediction of vaporized fuel. Fuel-rich flame-out is observed for the recirculation zone with the current model. As the heat transfer and the amount of air captured in the recirculation zone are competitive with respect to the mixture ratio and both increase with increasing A_p/A_{in}, this leads to an optimum value of A_p/A_{in}. At this optimum, the gas temperature reaches its maximum value. For the sustained combustion limit, no minimum value for A_p/A_t is found. Therefore, the latter limit may cross the non-sustained limit. Beyond the point of intersection, it is assumed that the combustor exhibits flame-out. It can be seen that the experimentally found flammability limits and the limits found with COPPEF coincide with the calculated limits for values of A_p/A_{in} lower than 4. For values of A_p/A_{in} larger than 4, the calculated limits deviate from the experimental limits.

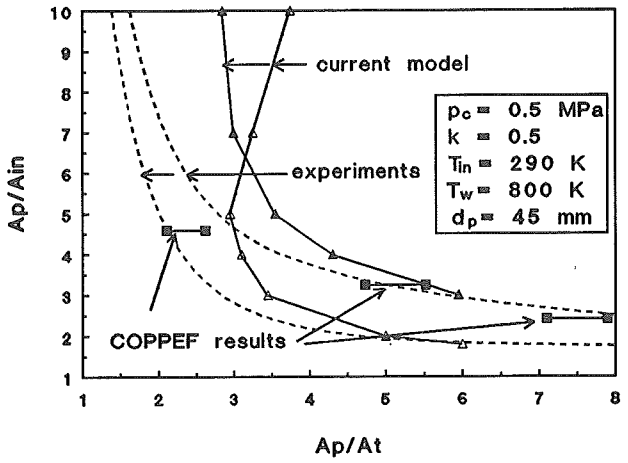

Figure 17: Calculated flammability limits, comparison with experimental results and results obtained with COPPEF[39].

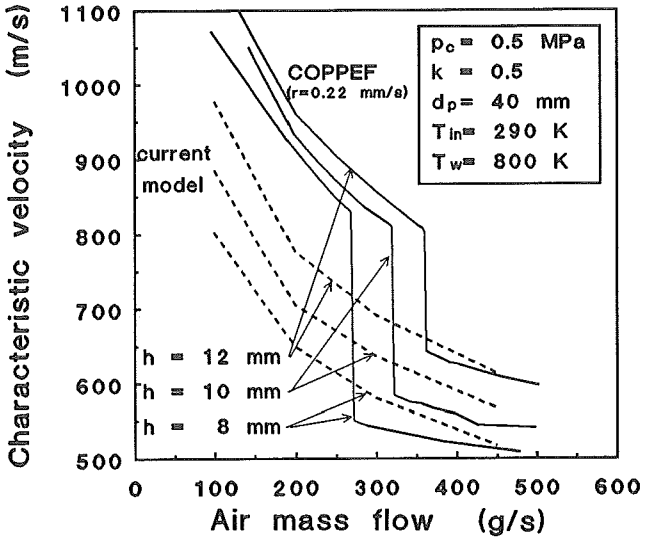

Figure 18: Calculated characteristic velocity as a function of the inlet air mass flow, comparison with results obtained with COPPEF[39].

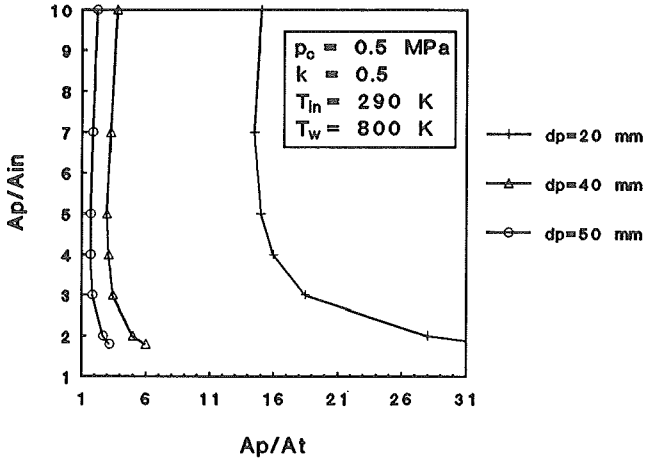

a: Effect of fuel port diameter.

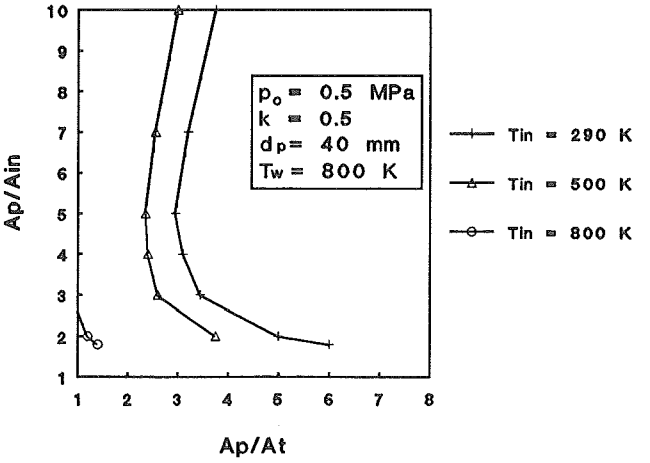

b: Effect of inlet temperature.

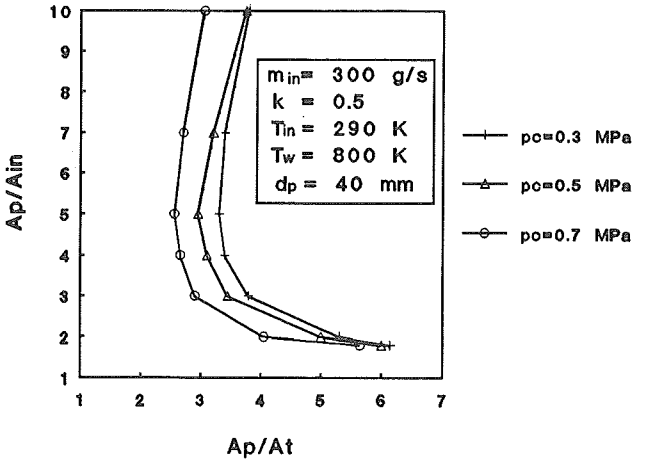

c: Effect of chamber pressure.

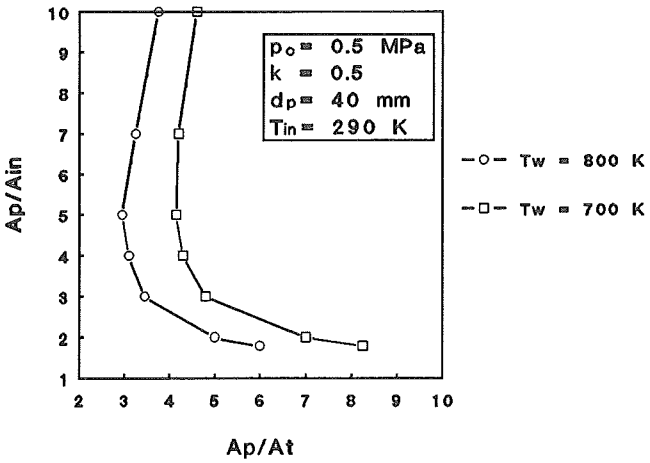

d: Effect of wall temperature.

Figure 19: Calculated non-sustained flammability limits.

The results from COPPEF[39] have been obtained by calculating the characteristic velocity c* as a function of the inlet air mass flow at fixed values of the fuel regression rate. A steep drop in the value of c* indicates combustor flame-out. When representing the results in this way, similar graphs are obtained. This is shown in figure 18. For the current model, no steep drop in the value of c* with increasing air mass flow is noticed. This is supported by the experimental results, which reveal a gradual transition from sustained to non-sustained. For the COPPEF results, a value

for c* at flame-out of 800 m/s is found. This is near the experimentally found critical value of 770 m/s.

In figure 19.a-d, the calculated non-sustained flammability limits are shown as a function of the fuel port diameter, the inlet temperature, the chamber pressure and the wall temperature, respectively. These trends show that the sustained area increases with increasing fuel port, increasing inlet temperature and increasing chamber pressure. At an inlet temperature of 800 K, sustained combustion is possible even for values of A_p/A_t = 1. A small region where non-sustained combustion is found is still present, however. A lower wall temperature is unfavourable for flammability. This is explained by the fact that for lower wall temperatures, more fuel is vaporized due to the smaller heat of gasification[38]. This leads to an unfavourable, more fuel rich mixture. The trends found for the effects of fuel port, inlet temperature and chamber pressure on the flammability limits are in agreement with the trends reported by other investigators[3-7].

The effect of the vortex shedding factor k on the flammability limits is shown in figure 20. The optimal flammability limit is found for k = 0.3 - 0.5. For higher and lower values of k, the sustained region becomes smaller. This is explained as follows. Increasing k means that more cold air is captured in the recirculation zone, by which a more favourable, less fuel rich, mixture ratio is obtained. However, increasing k also means a larger effect of the inlet air temperature on the initial temperature. As these effects are competitive, an optimum for the value of k is found.

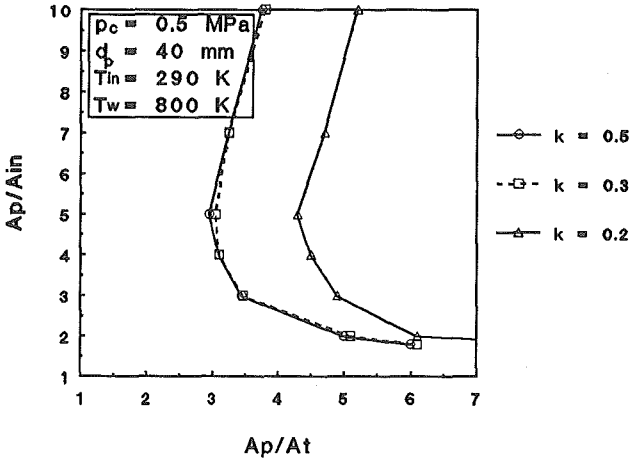

Figure 20: Calculated non-sustained flammability limits, effect of vortex shedding factor k.

V Conclusions and recommendations

The developed experimental method to determine the flammability limits of an SFRJ combustor with the PML-TNO/FAE-DUT ramjet test facility results in predicted flammability limits which agree with the predicted flammability limits, obtained from interpolation between literature values. A critical value of c* = 770 m/s for sustained experiments if found. This is close to the critical value of c* = 800 m/s, found with COPPEF.

The combustion process was observed to gradually improve from non-sustained to sustained, expressed by increasing values of c* and the combustion quality parameter ξ, defined in chapter III. The intermediate region is indicated as partially sustained and is characterized by combustion which is restricted to a part of the fuel grain. The findings that combustion behind the recirculation zone takes place for all experiments, exhibiting combustion in the recirculation zone is in agreement with the adopted flammability mechanism.

The self-ignition temperature T_{si} = 800 K, reported in literature, is in agreement with the experimental findings that no ignition has been achieved for theoretical ignition gas temperatures lower than 800 K. This is called the ignition limit of the SFRJ igniter/combustor combination.

The developed model, based on the adopted flammability mechanism and the vortex shedding model, shows trends that are in agreement with the results reported in literature. For k = 0.5 and low values of the step height, the experimental results agree with the calculational results. Probably the heat transfer to the solid fuel wall is overestimated by the current model. Proper modelling of the heat transfer and mixing processes should prove the model's reliability in the future.

Summarizing, it is concluded that the present model comprises the essential elements to predict flammability limits. It is concluded that the adopted flammability mechanism is essentially correct. This means that flammability of an SFRJ combustor is primarily governed by the Damköhler first number of the gases in the recirculation zone and the amount of heat, propagated to the flow behind the recirculation zone.

Acknowledgements

The work described in this paper was performed within the framework of the joint research programme carried out by the Faculty of Aerospace Engineering of the Delft University of Technology (FAE-DUT) and the Prins Maurits Laboratory of the Netherlands Organization for Applied Scientific Research (PML-TNO), to investigate the performance behaviour of a Solid Fuel Ramjet.

References

1. Myers, T.D., 'Special Problems of Ramjet with Solid Fuel', United Technologies/Chemical Systems Division.

2. Veraar, R.G., 'High Speed Airbreathing Propulsion Systems', PML-TNO/FAE-DUT Report PML 1988-C204.

3. Schulte, G., 'Fuel Regression and Flame Stabilization Studies of Solid-Fuel Ramjets', Journal of Propulsion and Power, vol. 2, number 4, 1986.

4. Netzer, A. and Gany, A., 'Burning and Flameholding Characteristics of a Miniature Solid Fuel Ramjet Combustor', AIAA-88-3044.

5. Netzer, A., 'Flameholding Limits and Combustion Characteristics of Different Solid Fuels in a Miniature Ramjet Engine', Collection of Figures, Technion-Israel Institute of Technology, Haifa, October 1987.

6. Wooldridge, R.C., 'An Experimental Investigation of the Ignition and Flammability Limits of Various Hydrocarbon Fuels in a Two-Dimensional Solid Fuel Ramjet', Master Thesis, Naval Postgraduate School, 1987, AD-A184 968.

7. Lips, H.R., Schmucker, R.H. and Witbracht, I.L., 'Experimental Investigations of a Solid Fuel Ramjet', Report DFVLR-FB 78-27, November 1978.

8. Nabity, J. and Walls, T., 'Side Dump Solid Fuel Ramjet Combustor Evaluation, AIAA-88-3072.

9. Schulte, G., Pein, R. and Högl, A., 'Temperature and Concentration Measurements in a Solid Fuel Ramjet Combustion Chamber', Journal of Propulsion and Power, March-April 1987.

10. Pitts, W.M., 'Importance of Isothermal Mixing Processes to the Understanding of Lift-Off and Blowout of Turbulent Jet Diffusion Flames', Combustion and Flame 76: 197-212 (1989).

11. Laan, F.H. van der and Timnat, Y.M., 'Chemical Rocket Propulsion', Lecture Series D-35 DUT, April 1985.

12. Elands, P.J.M., Korting, P.A.O.G., Dijkstra, F. and Wijchers, T., 'Combustion of Polyethylene in a Solid Fuel Ramjet a Comparison of Computational Results', AIAA-88-3043.

13. Zvuloni, R. Gany, A. and Levy, Y., 'Geometric Effects on the Combustion in Solid Fuel Ramjets', Collection of papers of the 28th Israel Annual Conference on Aviation and Astronautics, 1986.

14. Geld, C.W.M. van der, Korting, P.A.O.G. and Wijchers, T., 'Combustion of PMMA, PE and PS in a Ramjet', PML-TNO/FAE-DUT Report LR-514/PML 1987-C18.

15. Krall, K.M. and Sparrow, E.M., 'Turbulent Heat Transfer in the Separated, Reattached and Redeveloped Regions of a Circular tube', Journal of Heat Transfer (ASME), vol. 88 (1966) no 1, pg. 131-136.

16. Zemanick, P.P. and Dougall, R.S., 'Local Heat Transfer Downstreams of Abrupt Circular Channel Expansion', Journal of Heat Transfer (ASME), vol. 92 (1970) no1, pg. 53-60.

17. Geld, C.W.M. van der, 'On the Direct Simulation of Vortex Shedding', PML-TNO/FAE-DUT Report LR-513/PML 1987-C17

18. Kailasanath, K., Gardner, J.H., Oran, E.S. and Boris, J.P., 'Effects of Energy Release on High-Speed Flows in an Axisymmetric Combustor', AIAA-89-0385.

19. Kailasanath, K., Gardner, J., Boris, J. and Oran, E., 'Numerical Simulations of the Flowfield in a Central-Dump Ramjet Combustor I. Tests of the Model and Effects of Forcing', Naval Research Laboratory, NRL Memorandum Report 5832, July 1986.

20. Kailasanath, K., Gardner, J.H., Boris, J.P. and Oran, E.S., 'Numerical Simulations of Acoustic-Vortex Interactions in a Central-Dump Ramjet Combustor', Journal of Propulsion, vol. 3, number 6 1987.

21. Yu, K. Trouve, A., Keanini, R., Bauwens, L. and Daily, J., 'Low Frequency Pressure Oscillations in a Model Ramjet Combustor-The Nature of Frequency Selection', AIAA 89-0623.

22. Reuter, D.M., Hegde, U.G. and Zinn, B.T., 'Flowfield Measurements in an Unstable Ramjet Burner', AIAA-88-2855.

23. Poland, R.Y.C.M., 'Actieve Akoestische Resonantie in Ramjet Verbrandingskamers', Master Thesis FAE-DUT, July 1989.

24. Kuo, K.K., 'Principles of Combustion', John Wiley & Sons, New York, 1986.

25. Moore, W.J., 'Physical Chemistry', Longman House, Burnt Mill, Harlow, Essex, U.K., 1981.

26. Vos, J.B., 'The Calculation of Turbulent Reacting Flows with a Combustion Model Based on Finite Chemical Kinetics', Ph.D. Thesis, 1987.

27. Vos, J.B., 'Combustion Modelling in an SFCC and a Description of the KINETICS Computer Code', PML-TNO/FAE-DUT Report LR-481/PML 1986-C14.

28. Vos, J.B., 'The Calculation of Chemically Reacting Turbulent Boundary Layers by Means of Finite Chemical Kinetics', AIAA-86-1655.

29. Vos, J.B. Simulating an Ignition Pulse in Turbulent Reacting Flows Calculated with a Finite Chemical Kinetics Combustion Model', AIAA-87-1979.

30. Wilson, K.J., Schadow, K.C., Gutmark, E., Korting, P.A.O.G. and Dijkstra, F., 'Effect of Inlet Geometry on the Flow and Combustion Processes in a Solid Fuel Ramjet', Conference Proceedings, 31st Israel Annual Conference on Aviation and Astronautics, Haifa Israel, February 21-22 1990.

31. Jones, C.E., 'Investigations into the Variation of the Internal Ballistics of a Solid Fuel Ramjet through Combustor Design', Naval Postgraduate School, Monterey California, AD-769747, 1973.

32. Boaz, L.D., 'Internal Ballistics of Solid Fuel Ramjets', Naval Postgraduate School, Monterey California, AD-764491, 1973.

33. Korting, P.A.O.G., Geld, C.W.M. van der, Vos, J.B., Wijchers, T., Nina, M.N.R. and Schöyer, H.F.R., 'Combustion of PMMA in a Solid Fuel Ramjet', AIAA-86-1401.

34. Korting, P.A.O.G., 'Gebruik van het Gastoevoersysteem en de Vitiator voor de Vaste Brandstof Verbrandingskamer', PML-TNO/FAE-DUT Report LR-528/PML 1987-C103.

35. Schöyer, H.F.R. and Korting, P.A.O.G., 'A Sonic Control and Measuring Choke for the Precise Control and Measurements of Gas (Oxygen) Mass Flow Rates', PML-TNO/FAE-DUT Report LR-V02/PML 1984-C59.

36. Gordon, S. and McBride, B.J., 'Computer Program for Calculation of Complex Chemical Equilibrium Compositions, Rocket Performance, Incident and Reflected Shocks and Chapman-Jouguet Detonations', NASA SP-273, NASA Washington 1971.

37. Calzone, R.F., 'Thermodynamic Properties of a Reacting Gas', TNO/NLR/STORK Report AP GE TN 02 01 012, 1990.

38. Wilde, J.P. de, 'The Heat of Gasification of Polyethylene and Polymethylmethacrylate', PML-TNO/FAE-DUT Report PML 1988-C42.

39. Elands, P.J.M., Dijkstra, F. and Zandbergen, B.T.C., 'Experimental and Computational Flammability Limits in a Solid Fuel Ramjet', AIAA-90-1964.